The complex structure of SiIV regions of the Oe star λ Orionis

E. Danezis, M. Koutroumanou, E. Lyratzi, E. Theodossiou, M. Stathopoulou, D. Nikolaidis, A. Antoniou, C. Drakopoulos & A. Soulikias
University of Athens, School of Physics
Department of Astrophysics, Astronomy and Mechanics
Panepistimiopolis, Zografos 157 84
Athens – Greece

Abstract

In this paper we present a study of the SiIV resonance lines in UV of the Oe star λ Orionis, using spectrograms, taken by IUE, in different epochs. We reproduced the above mentioned lines by the model proposed by Danezis et al. (2003), which is based on the idea of independent density layers in the regions where the spectral lines that present SACs (DACs) are created. We calculated the apparent rotation (V_{rot}) and expansion/contraction velocities (V_{exp}) of these density regions, as well as their ξ value, which is an expression of the optical depth. We also present the relation among these parameters and their evolution with time.

Introduction

Schlesinger & Jenkins (1940) mention λ Orionis as a variable binary system with a spectral type Oe5. The two stars of the system, HR1879 and HR1889 have the same coordinates (a=5^h 29^m 38^s and δ=9° 52' for 1950) but with different apparent magnitudes m_1=3.66 and m_2=5.66 respectively. Jeffers et al. (1963) mention λ Orionis as a visually binary system with an early-type primary star and a fainter secondary one. The primary star's age and mass are t=8×10^6 years and 20M$_\odot$ (Iben 1967). The distance of λ Orionis from the Sun is 430 pc and its luminosity is L=10^5 L$_\odot$ (Panagia, 1973). Conti & Alschuler (1971) classified it as O8IIIe, but finally Walborn (1972) proposed the spectral type O8IIIf which implies the presence of emitting ionized He (λ 4686 Å), double ionized NIII (λ 5696 Å) and probably emission by ionized CIII (λ 5696 Å). Lamers et al. (1979) studying the intensity of FeII (λ 2548 Å) and FeIII (λ 2078 Å), as well as the visual region of the star's spectrum, came to the conclusion that λ Orionis is a normal star with an irregular spectrum in UV. They emphasised that the shape of the FeII spectral lines is rather weak and the MgII spectral region may emit. Lindros (1985) included λ Orionis in a project about visually double stars and proposed that it may belong to a triple system. According to the observations by Lindros, the primary star of the system is a O8III spectral type, the secondary B0V and the third accompanying is an F8V. Theodossiou & Danezis (1991) studying 500 early type stars including λ Orionis, concluded that its effective temperature is T_{eff}=35.000±2.300 ºK.

Danezis et al. (1993) studied the CIII, NIII, NIV, AlII, FeII and FeV spectral lines in the UV spectra of λ Orionis and found that: a) there are not any spectral features implying that the star belongs to a binary system, with a secondary B component, b) the spectral lines of ions with ionization potential up to 30 eV present apparent radial velocities about 40 km/s, c) the FeV (55 eV) spectral lines are the result of the composition of two components with apparent radial velocities 32 km/s

and 5 km/s, while the radial velocity of the regions where the NV lines are created is about 8 km/s.

In this paper we present a study of the regions where the SiIV resonance lines ($\lambda\lambda$ 1393.755, 1402.77 Å) are created, in the gaseous envelope of λ Ori, for the time period between 1981 and 1992. For our study we use the proposed by Danezis et al. (2003) model for the structure of the SACs regions in the early type atmospheres, which we describe briefly in the next paragraph.

The model: Mathematical expression

Considering an area of gas consisting of i independent absorbing shells followed by a shell that both absorbs and emits and an outer shell of general absorption, we conclude to the function:

$$I_\lambda = \left[I_{\lambda 0} \prod_i \exp\{-L_i \xi_i\} + S_{\lambda e}\left(1 - \exp\{-L_e \xi_e\}\right) \right] \exp\{-L_g \xi_g\}$$

where: **$I_{\lambda 0}$:** the initial radiation intensity,

L_i, L_e, L_g: are the distribution functions of the absorption coefficients $k_{\lambda i}$, $k_{\lambda e}$, $k_{\lambda g}$ respectively. Each L depends on the values of the apparent rotation velocity as well as of the radial expansion/contraction velocity of the density shell, which forms the spectral line (V_{rot}, V_{exp}),

$\xi = \int_0^s \Omega \rho ds$ is an expression of the optical depth τ, where Ω: an expression of k_λ and has the same units as k_λ,

$S_{\lambda e}$: the source function, which, at the moment when the spectrum is taken, is constant and

$L = \sqrt{1 - \cos^2 \theta_0}$ if $\cos \theta_0 < 1$ and $L = 0$ if $\cos \theta_0 \geq 1$,

where $\cos \theta_0 = \dfrac{-\lambda_0 + \sqrt{\lambda_0^2 + 4\Delta\lambda^2}}{2\Delta\lambda z_0}$, where $2\theta_0$ is the angular width of the equatorial disk of matter, λ_0 is the wavelength of the center of the spectral line and $\lambda_0 = \lambda_{lab} + \Delta\lambda_{exp}$, with λ_{lab} being the laboratory wavelength of the spectral line produced by a particular ion and $\Delta\lambda_{exp}$ the radial Doppler shift and $\dfrac{\Delta\lambda_{exp}}{\lambda_{lab}} = \dfrac{V_{exp}}{c}$.

$z_0 = \dfrac{V_{rot}}{c}$, where V_{rot} is the apparent rotation velocity of the i density shell of matter and

$\Delta\lambda = |\lambda_i - \lambda_0|$, where the values of λ_i are taken in the wavelength range we want to reproduce.

The spectral line's profile, which is formed by the i density shell of matter, must be accurately reproduced by the function $e^{-L_i \xi_i}$ by applying the appropriate values of V_{roti}, V_{expi} and ξ_i. Using the best model's fit for a complex spectral line, we can calculate the apparent expansion/contraction (V_{expi}) velocity, the apparent rotation velocity (V_{roti}) and an expression of the optical depth (ξ_i) of the region in which the main spectral line and its SACs are created.

Data

The data we used are the 13 IUE spectra taken by the Villafranca Satellite Tracking Station of the European Space Agency (VILSPA) database. Our data are presented in table 1.

Table 1	
Camera	**Date**
Swp 15295	20/10/1981
Swp 15331	20/11/1981
Swp 17901	09/09/1982
Swp 17968	15/09/1982
Swp 18096	24/09/1982
Swp 35944	05/04/1989
Swp 46159	08/11/1992
Swp 46177	09/11/1992
Swp 46196	10/11/1992
Swp 46216	11/11/1992
Swp 46237	12/11/1992
Swp 46245	12/11/1992
Swp 46253	13/11/1992

Figures

In figures 1 and 2 we present the SiIV lines' fittings of the 13 studied spectra of λ Orionis. The thick line presents the observed spectral line's profile and the thin one the model's fit. The dashed lines indicate the laboratory wavelengths of the SiIV resonance lines at λλ 1393.755, 1402.77 Å.

Figure 1

4

Swp 46159
8/11/1992

Swp 46177
9/11/1992

Swp 46196
10/11/1992

Swp 46216
11/11/1992

Swp 46237
12/11/1992

Swp 46245
12/11/1992

Swp 46253
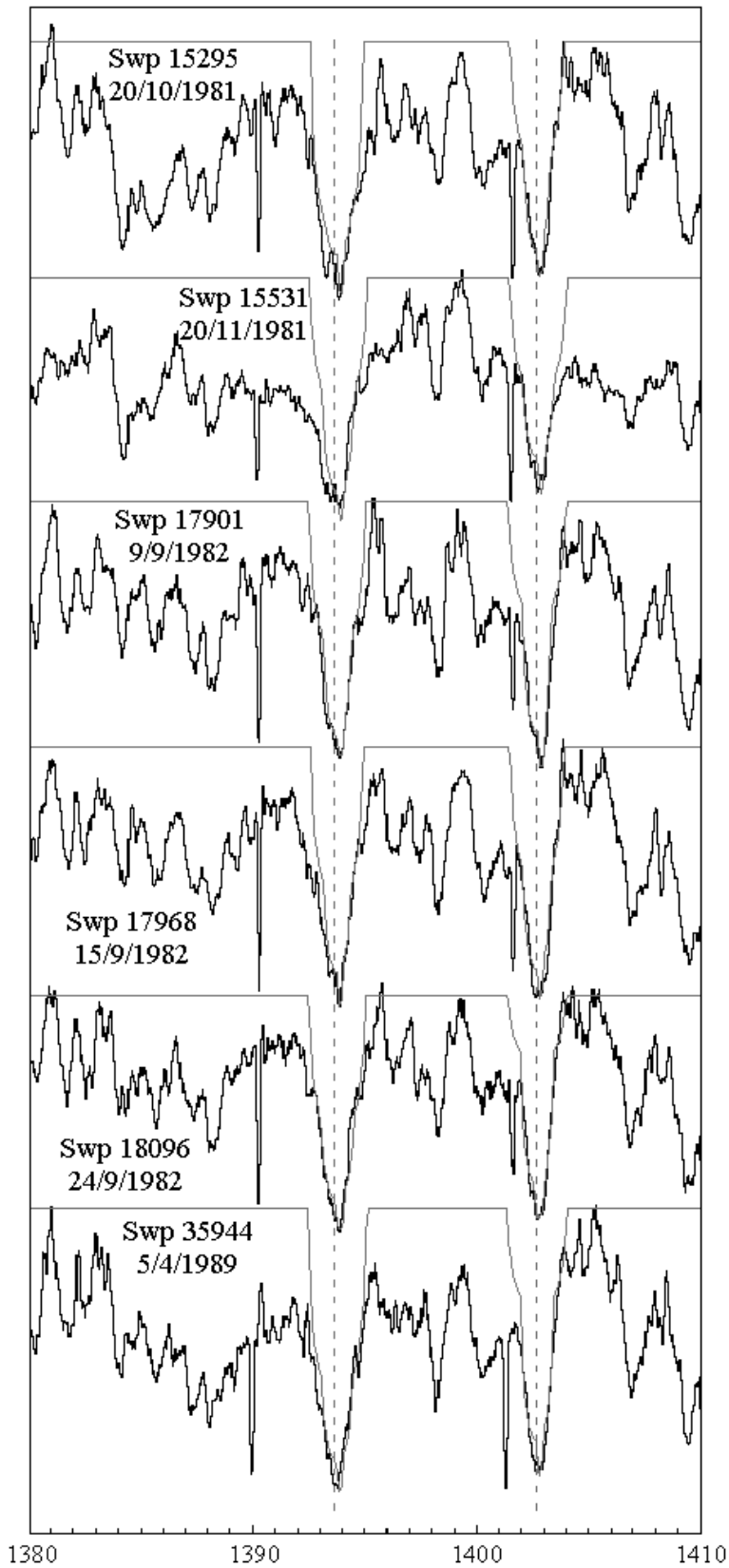13/11/1992

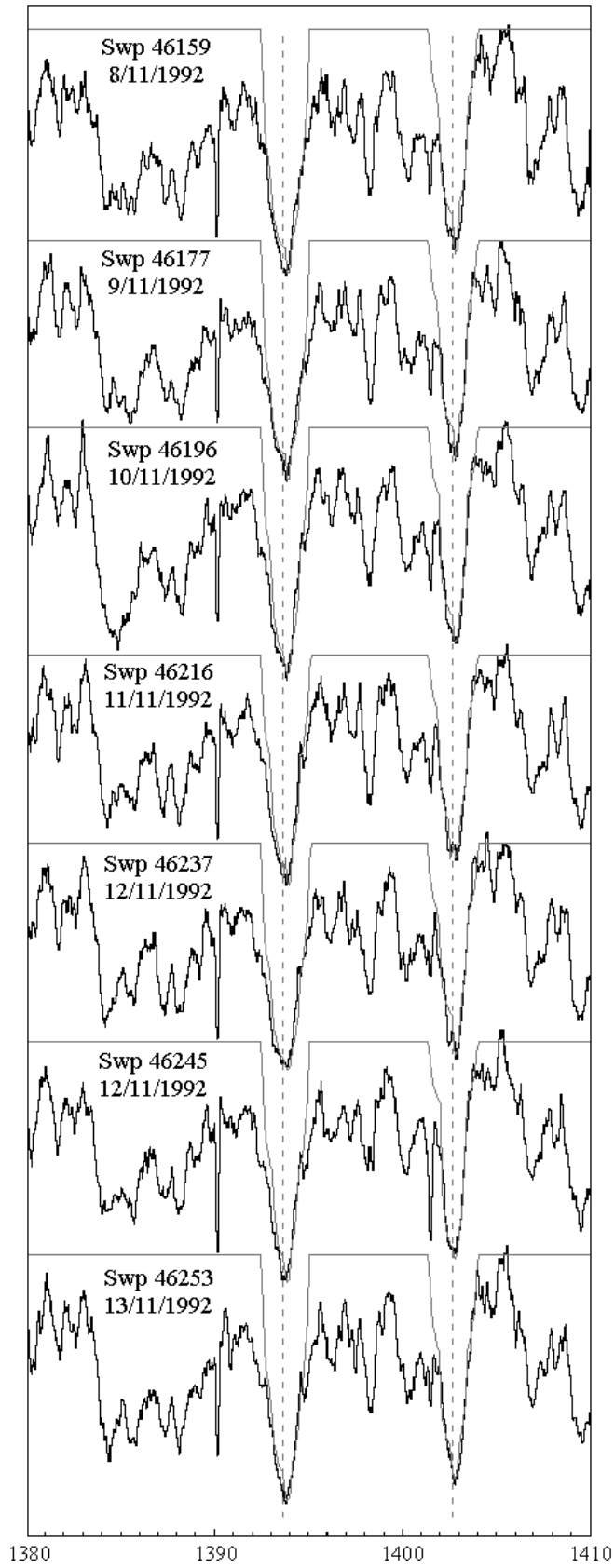1380   1390   1400   1410

Figure 2

Tables

In table 2 we present the apparent radial velocities (V_{exp}), the apparent rotation velocities (V_{rot}), the expression of the optical depth (ξ) (multiplied by 10) and an expression of the absorbed energy ($V_{rot}\xi$) (multiplied by 10), for each of the SiIV resonance lines and for each Satellite Absorption Component (SAC), independently. In the last column we present an expression of the overall absorbed energy which derives from both of the doublet's lines and their satellite components ($\Sigma(V_{rot}\xi)$) (multiplied by 10).

As many of the studied spectra have been taken in short time periods (about a month) and as no important variations are observed in such short periods, we have extracted the mean values of the above mentioned parameters.

Thus, in table 3 we present the mean values of the apparent radial velocities (V_{exp}), the apparent rotation velocities (V_{rot}) and the expression of the optical depth (ξ) (multiplied by 10) of both of the doublet's lines, for each satellite component independently and for all the spectra taken in one year periods. In the last column we present the mean values of the expression of the overall absorbed energy which derives from both of the doublet's lines and their satellite components, for all the spectra taken in one year periods ($\Sigma\Sigma(V_{rot}\xi)$) (multiplied by 10).

At this point we would like to point out that the calculated values of the apparent rotation and expansion/contraction velocities correspond to the regions, where the Satellite Absorption Components (SACs) are created, and not to the star. Specifically, these values correspond to the density regions (blobs, puffs, bubbles) which result when streams of matter are twisted and form strings that produce blobs, puffs or bubbles.

<table>
<thead>
<tr><th colspan="11">Table 2</th></tr>
<tr><th rowspan="2">Camera</th><th rowspan="2">Component</th><th colspan="4">λ=1393.755 Å</th><th colspan="4">λ=1402.77 Å</th><th rowspan="2">$\Sigma(V_{rot}\xi)$</th></tr>
<tr><th>V_{exp}</th><th>V_{rot}</th><th>ξ</th><th>$V_{rot}\xi$</th><th>V_{exp}</th><th>V_{rot}</th><th>ξ</th><th>$V_{rot}\xi$</th></tr>
</thead>
<tbody>
<tr><td rowspan="3">Swp 15295</td><td>a</td><td>0</td><td>121</td><td>0.54</td><td>65</td><td>0</td><td>121</td><td>2.44</td><td>259</td><td rowspan="3">2142</td></tr>
<tr><td>b</td><td>36</td><td>35</td><td>1.73</td><td>61</td><td>36</td><td>37</td><td>1.67</td><td>62</td></tr>
<tr><td>c</td><td>0</td><td>250</td><td>4.40</td><td>1100</td><td>0</td><td>250</td><td>2.38</td><td>596</td></tr>
<tr><td rowspan="3">Swp 15331</td><td>a</td><td>0</td><td>151</td><td>2.90</td><td>438</td><td>0</td><td>150</td><td>2.00</td><td>300</td><td rowspan="3">2314</td></tr>
<tr><td>b</td><td>29</td><td>32</td><td>1.48</td><td>47</td><td>34</td><td>33</td><td>1.48</td><td>49</td></tr>
<tr><td>c</td><td>0</td><td>270</td><td>2.97</td><td>802</td><td>0</td><td>270</td><td>2.51</td><td>678</td></tr>
<tr><td rowspan="3">Swp 17901</td><td>a</td><td>0</td><td>132</td><td>2.48</td><td>327</td><td>0</td><td>132</td><td>3.08</td><td>407</td><td rowspan="3">2175</td></tr>
<tr><td>b</td><td>38</td><td>40</td><td>0.89</td><td>36</td><td>49</td><td>38</td><td>1.66</td><td>63</td></tr>
<tr><td>c</td><td>0</td><td>270</td><td>2.84</td><td>767</td><td>0</td><td>270</td><td>2.13</td><td>575</td></tr>
<tr><td rowspan="3">Swp 17968</td><td>a</td><td>0</td><td>130</td><td>2.00</td><td>260</td><td>0</td><td>130</td><td>2.22</td><td>289</td><td rowspan="3">1971</td></tr>
<tr><td>b</td><td>27</td><td>24</td><td>1.43</td><td>34</td><td>34</td><td>27</td><td>1.14</td><td>31</td></tr>
<tr><td>c</td><td>0</td><td>250</td><td>2.86</td><td>715</td><td>0</td><td>250</td><td>2.57</td><td>643</td></tr>
<tr><td rowspan="3">Swp 18096</td><td>a</td><td>0</td><td>156</td><td>2.14</td><td>334</td><td>0</td><td>154</td><td>3.44</td><td>530</td><td rowspan="3">2251</td></tr>
<tr><td>b</td><td>29</td><td>50</td><td>1.36</td><td>68</td><td>26</td><td>52</td><td>1.43</td><td>74</td></tr>
<tr><td>c</td><td>0</td><td>270</td><td>3.25</td><td>878</td><td>0</td><td>270</td><td>1.36</td><td>367</td></tr>
<tr><td rowspan="3">Swp 35944</td><td>a</td><td>0</td><td>149</td><td>1.95</td><td>291</td><td>0</td><td>149</td><td>3.19</td><td>475</td><td rowspan="3">2387</td></tr>
<tr><td>b</td><td>27</td><td>30</td><td>1.36</td><td>41</td><td>28</td><td>30</td><td>1.36</td><td>41</td></tr>
<tr><td>c</td><td>0</td><td>280</td><td>3.73</td><td>1044</td><td>0</td><td>280</td><td>1.77</td><td>496</td></tr>
<tr><td rowspan="3">Swp 46159</td><td>a</td><td>0</td><td>167</td><td>1.89</td><td>316</td><td>0</td><td>165</td><td>2.87</td><td>474</td><td rowspan="3">2558</td></tr>
<tr><td>b</td><td>36</td><td>36</td><td>1.52</td><td>55</td><td>36</td><td>36</td><td>1.86</td><td>67</td></tr>
<tr><td>c</td><td>0</td><td>270</td><td>4.27</td><td>1153</td><td>0</td><td>270</td><td>1.83</td><td>494</td></tr>
<tr><td rowspan="3">Swp 46177</td><td>a</td><td>0</td><td>169</td><td>2.01</td><td>340</td><td>0</td><td>165</td><td>3.54</td><td>592</td><td rowspan="3">2824</td></tr>
<tr><td>b</td><td>31</td><td>25</td><td>1.89</td><td>47</td><td>36</td><td>27</td><td>1.83</td><td>49</td></tr>
<tr><td>c</td><td>0</td><td>270</td><td>4.82</td><td>1301</td><td>0</td><td>270</td><td>1.83</td><td>494</td></tr>
<tr><td rowspan="3">Swp 46196</td><td>a</td><td>0</td><td>161</td><td>3.21</td><td>517</td><td>0</td><td>159</td><td>3.27</td><td>520</td><td rowspan="3">2593</td></tr>
<tr><td>b</td><td>27</td><td>39</td><td>1.32</td><td>51</td><td>34</td><td>35</td><td>1.26</td><td>44</td></tr>
<tr><td>c</td><td>0</td><td>270</td><td>3.65</td><td>986</td><td>0</td><td>270</td><td>1.76</td><td>475</td></tr>
<tr><td rowspan="3">Swp 46216</td><td>a</td><td>0</td><td>170</td><td>3.03</td><td>515</td><td>0</td><td>170</td><td>2.97</td><td>505</td><td rowspan="3">2363</td></tr>
<tr><td>b</td><td>42</td><td>36</td><td>1.70</td><td>61</td><td>41</td><td>36</td><td>1.58</td><td>57</td></tr>
<tr><td>c</td><td>0</td><td>280</td><td>2.91</td><td>815</td><td>0</td><td>270</td><td>1.52</td><td>410</td></tr>
<tr><td rowspan="3">Swp 46237</td><td>a</td><td>0</td><td>165</td><td>2.44</td><td>403</td><td>0</td><td>163</td><td>2.50</td><td>405</td><td rowspan="3">2476</td></tr>
<tr><td>b</td><td>31</td><td>48</td><td>0.60</td><td>29</td><td>36</td><td>48</td><td>1.79</td><td>86</td></tr>
<tr><td>c</td><td>0</td><td>280</td><td>3.75</td><td>1050</td><td>0</td><td>280</td><td>1.79</td><td>501</td></tr>
<tr><td rowspan="3">Swp 46245</td><td>a</td><td>0</td><td>140</td><td>2.54</td><td>356</td><td>0</td><td>140</td><td>4.02</td><td>563</td><td rowspan="3">2266</td></tr>
<tr><td>b</td><td>27</td><td>37</td><td>1.36</td><td>50</td><td>32</td><td>37</td><td>0.65</td><td>24</td></tr>
<tr><td>c</td><td>0</td><td>270</td><td>3.43</td><td>926</td><td>0</td><td>270</td><td>1.42</td><td>383</td></tr>
<tr><td rowspan="3">Swp 46253</td><td>a</td><td>0</td><td>161</td><td>2.00</td><td>322</td><td>0</td><td>160</td><td>2.44</td><td>390</td><td rowspan="3">2626</td></tr>
<tr><td>b</td><td>27</td><td>49</td><td>1.44</td><td>71</td><td>26</td><td>50</td><td>1.44</td><td>72</td></tr>
<tr><td>c</td><td>0</td><td>270</td><td>4.06</td><td>1096</td><td>0</td><td>270</td><td>2.50</td><td>675</td></tr>
</tbody>
</table>

Table 3					
Date	Component	V_{exp} (km/s)	V_{rot} (km/s)	ξ	$\Sigma\Sigma(V_{rot}\xi)$
1981	a	0	136	1.97	2228
	b	34	34	1.59	
	c	0	260	3.07	
1982	a	0	139	2.56	2132
	b	34	39	1.32	
	c	0	263	2.50	
1989	a	0	149	2.57	2387
	b	28	30	1.36	
	c	0	280	2.75	
1992	a	0	161	2.77	2529
	b	33	39	1.45	
	c	0	272	2.82	

Diagrams and Conclusions
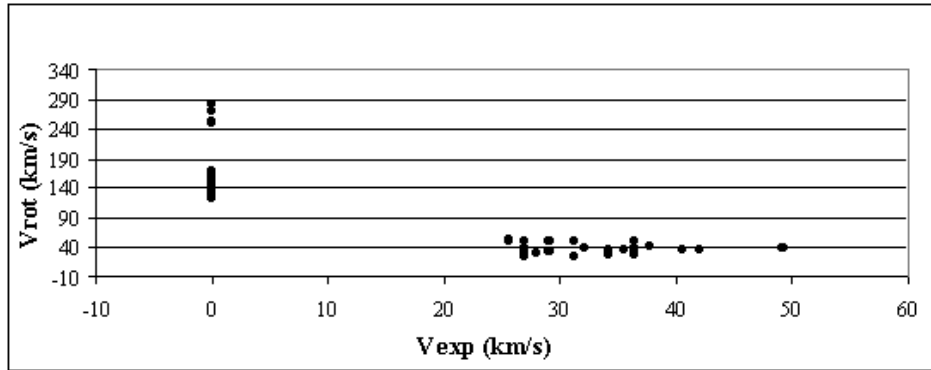
Diagram 1: (Data from table 1) Rotation velocities (V_{rot}) as a function of the expansion velocities (V_{exp}). One can see that two levels of V_{exp} are present, one of 0 km/s and another between 26 to 50 km/s. When V_{exp}=0, two levels of V_{rot} appear, one of about 150 km/s and another of about 270 km/s. The three levels of V_{rot} appear clearly in diagram 3. When V_{exp} lies between 26 and 50 km/s, V_{rot} is about 40 km/s.
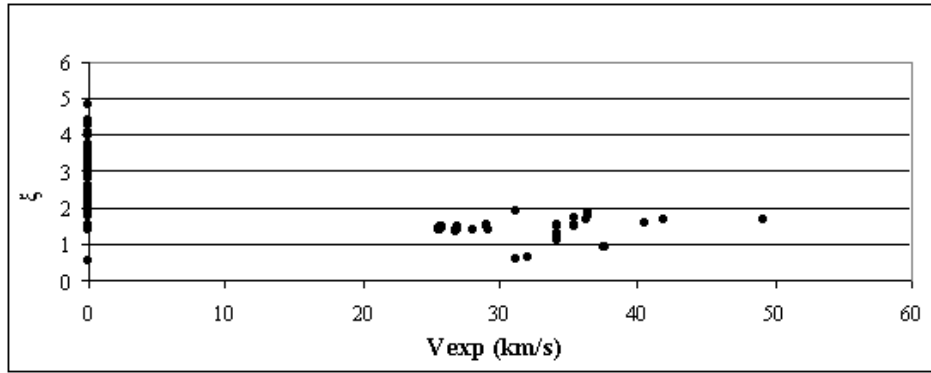
Diagram 2: (Data from table 1) The expression of the optical depth (ξ) as a function of the expansion velocity (V_{exp}). The two levels of V_{exp} appear clearly. When $V_{exp}=0$ km/s, the values of ξ lie between 0.05 and 0.5. For the second level of V_{exp} the values of ξ lie between 0.05 and 0.2.
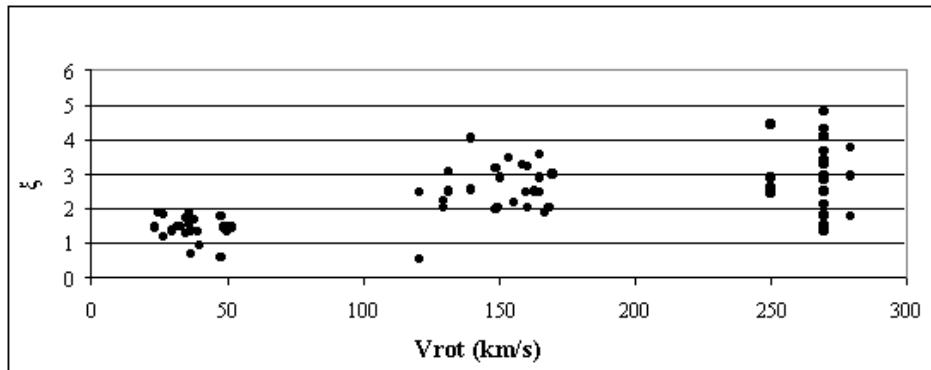
Diagram 3: (Data from table 1) The expression of the optical depth (ξ) as a function of the rotation velocity (V_{rot}), for all the SACs. The three levels of V_{rot} which lie around the values of 40, 150 and 275 km/s appear clearly. In the case of 40 km/s the values of ξ lie between 0.05 and 0.2. In the case of 150 km/s the values of ξ lie between 0.2 and 0.4. In the case of 275 km/s the values of ξ lie between 0.15 and 0.5.
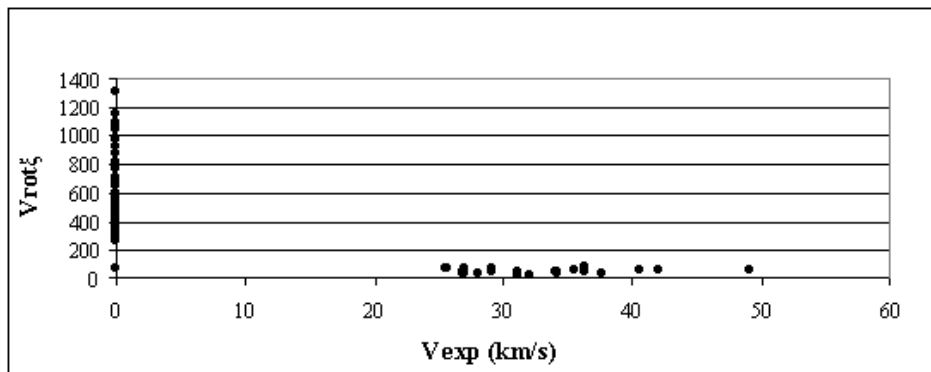
Diagram 4: (Data from table 1) An expression of the absorbed energy ($V_{rot}\xi$) as a function of the expansion velocity (V_{exp}). When $V_{exp}=0$, the values of $V_{rot}\xi$ lie between 24 and 1250. The second level of V_{exp} between 26 and 50 km/s correspond to almost constant values of $V_{rot}\xi$ around 35.

9
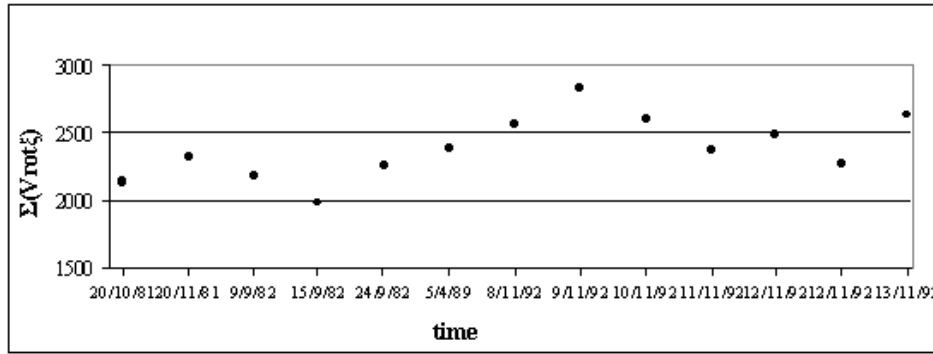
Diagram 5: (Data from table 1) Variation of $\Sigma(V_{rot}\xi)$ as a function of the date. $\Sigma(V_{rot}\xi)$ is an expression of the overall absorbed energy in the regions where the satellite components of both of the doublets lines are created.
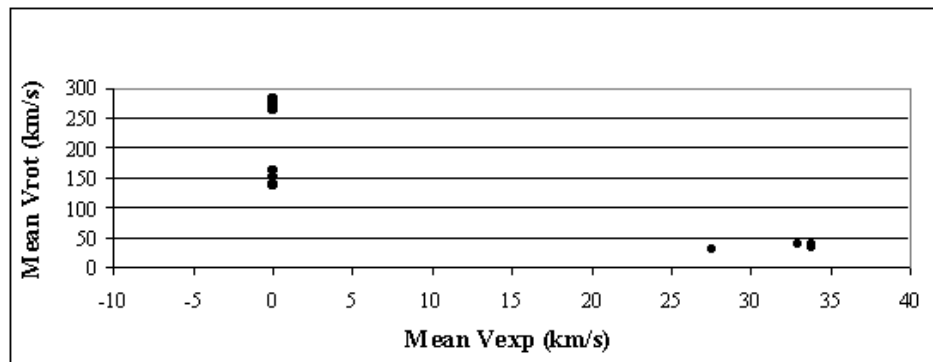
Diagram 6: (Data from table 2) Mean values of V_{exp} as a function of V_{rot}. One can see that two levels of expansion velocity are present, one of 0 km/s and another between 29 to 34 km/s. When V_{exp}=0 there appear two levels of V_{rot}, one about 150 km/s and another about 270 km/s. When V_{exp} lies between 29 and 34 km/s, V_{rot} is about 40 km/s.
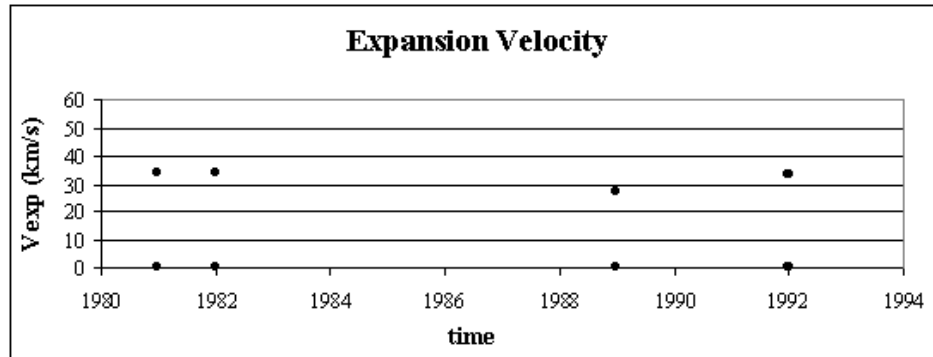
Diagram 7: (Data from table 2) Variation of the two levels of the mean apparent V_{exp} as a function of the date. The two levels of V_{exp} remain almost constant around the values of 0 and 34 km/s.

10
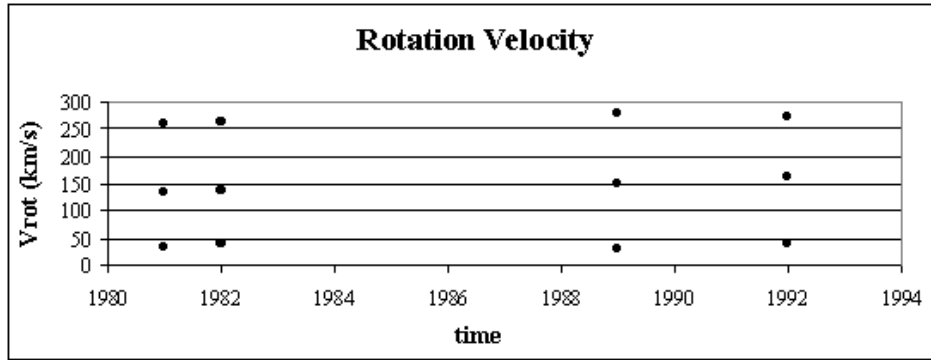
Diagram 8: (Data from table 2) Variation of the two levels of the mean apparent V_{rot} as a function of the date. The three levels of V_{rot} remain almost constant around the values of 40, 150 and 270 km/s.
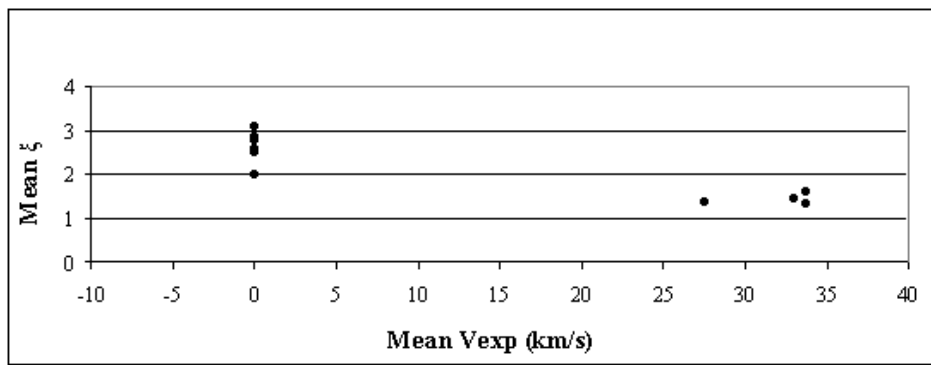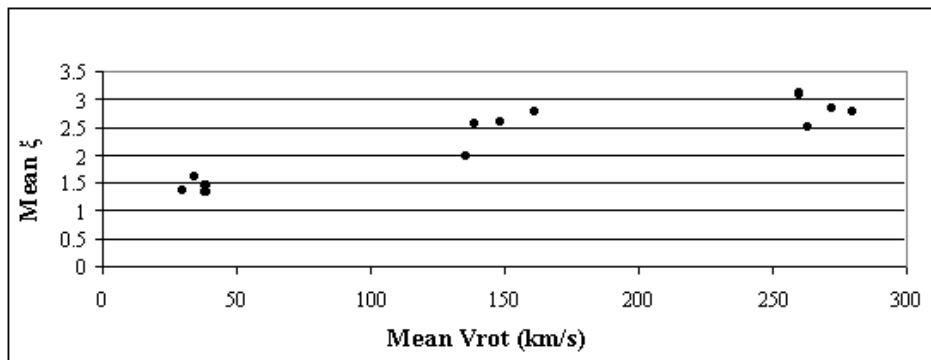

Diagram 9: (Data from table 2) The mean values of the expression of the optical depth (ξ) as a function of the mean values of the expansion velocity (V_{exp}). The two levels of V_{exp} appear clearly. When V_{exp}=0 km/s, the values of ξ lie between 0.2 and 0.34. For the second level of V_{exp} the values of ξ lie between 0.1 and 0.15.

Diagram 10: (Data from table 2) The mean values of the expression of the optical depth (ξ) as a function of the mean values of the rotation velocity (V_{rot}), for all the SACs. The three levels of V_{rot} which lie around the values of 40, 150 and 275 km/s appear clearly. In the case of 40 km/s the values of ξ lie between 0.1 and 0.16. In the case of 150 km/s the values of ξ lie between 0.2 and 0.325. In the case of 275 km/s the values of ξ lie between 0.25 and 0.31.
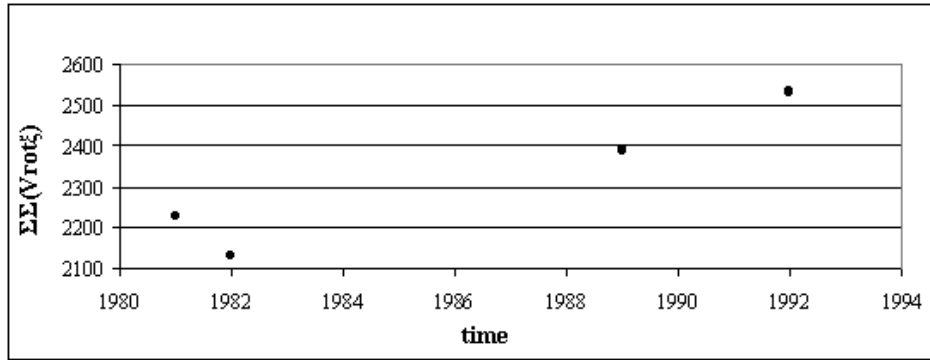
11

Diagram 11: (Data from table 2) Variation of $\Sigma\Sigma(V_{rot}\xi)$ as a function of the date. From 1981 to 1992, we observe an important increase of the expression of the overall absorbed energy in the region where the SiIV resonance lines are created.

References

Conti, P.S. & Alschuler, W.R.:1971, ApJ, 170, 325

Danezis, E., Thedossiou, E. & Laskarides, P. G.: 1993 *The UV spectrum of λ Orionis,* Proceedings of the 6th Hellenic Physics Conference. Komotini (in Greek)

Danezis, E., Nikolaidis, D., Lyratzi, V., Stathopoulou, M., Theodossiou, E., Kosionidis, A., Drakopoulos, C., Christou G. & Koutsouris, P.: 2003, Ap&SS, 284, 1119

Iben, I.:1967, Ann. Rev. A&A 5, 571

Jeffers, H. M., van de Box, W. H. & Greeby, F. M.: 1963, "Index Catalogue of Visual Double Star", Publ. Link Obs. 21

Kelly, R. L. 1987, Atomic and Ionic Spectrum Lines below 2000 A. Hydrogen through Krypton. Part I, II, III. Physical and Chemical Reference Data Vol. 16, Suppl. No.1

Lamers, H. J. G. L. M., Faraggiana, R. & Burger, M.: 1979, A&A, 79, 230

Lindros, K. P.: 1985, A&AS, 60, 183

Moore, C. E.: 1962, NBS Circ. 488, 1-4

Panagia, N.: 1973, ApJ, 78, 929

Schlesinger, F. & Jenkins, L. F.: 1940, QB6, S34

Theodossiou, E. & Danezis, E.: 1991, Ap&SS, 183, 91

Walborn, N. R.:1972, ApJ, 77, 312